Current status of ^{90}Sr Čerenkov calibration sources for SNO

R. J. Boardman
Nuclear Physics Laboratory
Keble Road, Oxford
United Kingdom

May 7, 1992

Čerenkov sources

In this report the simulation and construction of Čerenkov sources, based on the encapsulation of a radioactive beta source inside a sphere of borosilicate glass, are described. These sources are required to have several properties which enable them to be used as 'calibration sources', for both the SNO detector and the measurement of photomultiplier photon counting efficiency.

An important requirement of such a source is that it must be constructed in a way which enables a reliable computation of its light output to be performed. If the source is to be used for calibration then it should not deviate from the computed intensity with time. As with every radioactive source, it is required to be robust and to have minimal surface contamination. If such a source were to be used to calibrate the response of photomultipliers in the SNO detector, these latter constraints become critical. The source must also radiate light of appropriate intensity so that the photomultipliers which detect the photons count at an acceptable rate. In practice this is achieved by altering the amount of beta decay activity in the source.

The choice of radioisotope is dictated by the requirements of long half-life and no γ transitions. Furthermore, the radioisotope should be available in an appropriate chemical form not only for encapsulation, but also to enable an accurate determination of its specific activity. Three isotopes have been suggested, namely ^{204}Tl, ^{90}Sr, and ^{32}P. The latter is rejected for this work due to its short half-life of only 14.3 days, and ^{204}Tl is also unsuitable as the beta decay electrons have an end-point of only 775 keV. ^{36}Cl, with an end-point energy of 709 keV, is similarly unsuitable, as beta decays with end-point energies of about 700 keV produce an order of magnitude less Čerenkov radiation than ^{90}Sr, for similar amounts of activity.

To improve the accuracy of a Čerenkov source simulation, it is important to consider the ease of computation of the beta decay spectra of candidate isotopes, and also to select decay nuclei that do not have associated γ transitions. With modern simulation techniques, such as the EGS4 Monte Carlo, this restriction is not quite so critical as the Čerenkov yield from Compton scattered electrons can be estimated. However, this will make the simulation more complex, and for reasons of radiation safety, decays producing a significant γ-ray flux are unsuitable. For these reasons the isotope ^{90}Sr is used in all the sources described in this work. ^{90}Sr, and its daughter ^{90}Y, both have beta decay transitions which are γ free, and their first-forbidden beta spectra are relatively easy to calculate. The decay scheme is shown in figure 1. The end-point of the ^{90}Y beta spectrum is quite high, 2.28 MeV, and therefore
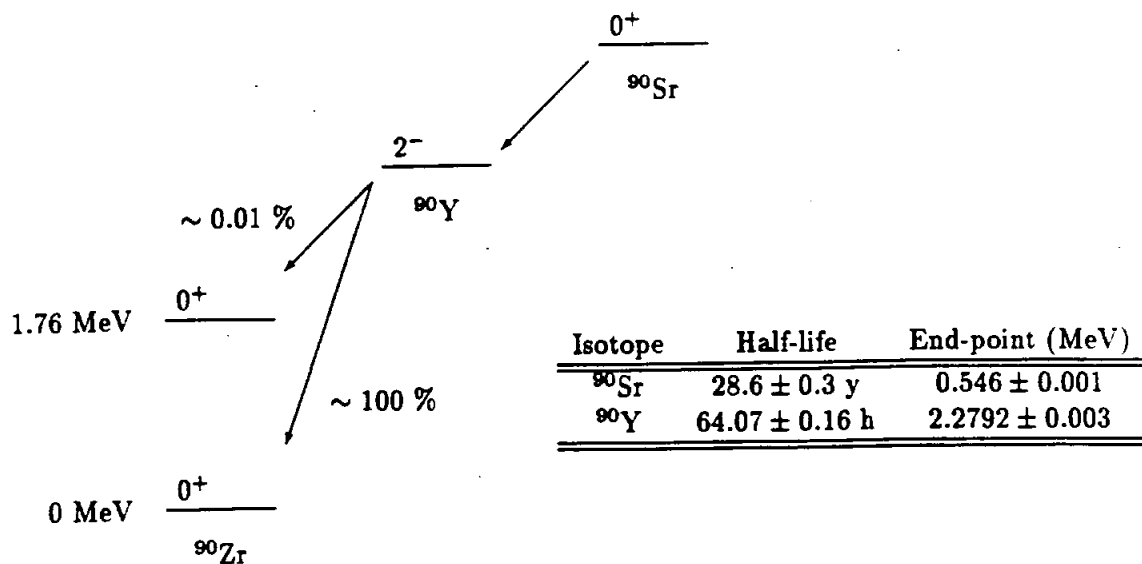
0^+

^{90}Sr

2^-

~ 0.01 % ^{90}Y

1.76 MeV 0^+

~ 100 %

Isotope	Half-life	End-point (MeV)
^{90}Sr	28.6 ± 0.3 y	0.546 ± 0.001
^{90}Y	64.07 ± 0.16 h	2.2792 ± 0.003

0 MeV 0^+

^{90}Zr

Figure 1: The beta decay of ^{90}Sr and ^{90}Y.

the yield of Čerenkov radiation per beta decay is relatively high. The half-life of ^{90}Sr is conveniently long, being approximately 28 years.

Encapsulation materials

In this section the optical and physical properties of the materials used to encapsulate the ^{90}Sr are described. For the purposes of simulation, the density, refractive index and optical transmission of the encapsulation material should be known accurately. These properties are significant as the material used to construct a source serves not only for encapsulation, but also as the Čerenkov medium for the stopping electrons. The optical transmission of all the media used are measured, so that a reliable estimate of the spectral luminance of the source can be made. The material currently used for encapsulation is borosilicate glass, filled with radio-active nuclide dissolved in high-purity water. Borosilicate glass has a pronounced short wavelength cut-off, which is usually quite sharp, but it is inevitable that the bulk attenuation length is reduced before the cut-off point. This introduces a source of error into simulations of the spectral intensity of the Čerenkov sources used. The approach taken in this work is to accept that this is inevitable and ensure that these sources are always used in a way which is not sensitive to the bulk transmission at short wavelengths. If such a source were to be used in the heavy water, then a glass wall is probably acceptable, but in the light water quartz would be required.

The measurements of optical transmission, shown in figure 2, were performed used a Perkin-Elmer Lambda-9 spectrophotometer, which can measure transmission over the range of wavelengths of interest, between about 300 and 700 nm . Several samples of glass and many of acrylic have been tested, and some typical raw data, uncorrected for Fresnel reflections.

The solid line of figure 2 shows the transmission of a 4 mm thick sample of Schott 8246. The dotted line in the figure shows the transmission of a sample of ICI 'Perspex' acrylic, of thickness 12.7 mm (1/2 inch). This material has had a uv-stabilizer added to the monomer to ensure that the acrylic is not damaged by ultra-violet radiation. The effect of this additive is to attenuate ultra-violet light with wavelengths shorter than about 370 nm. This material
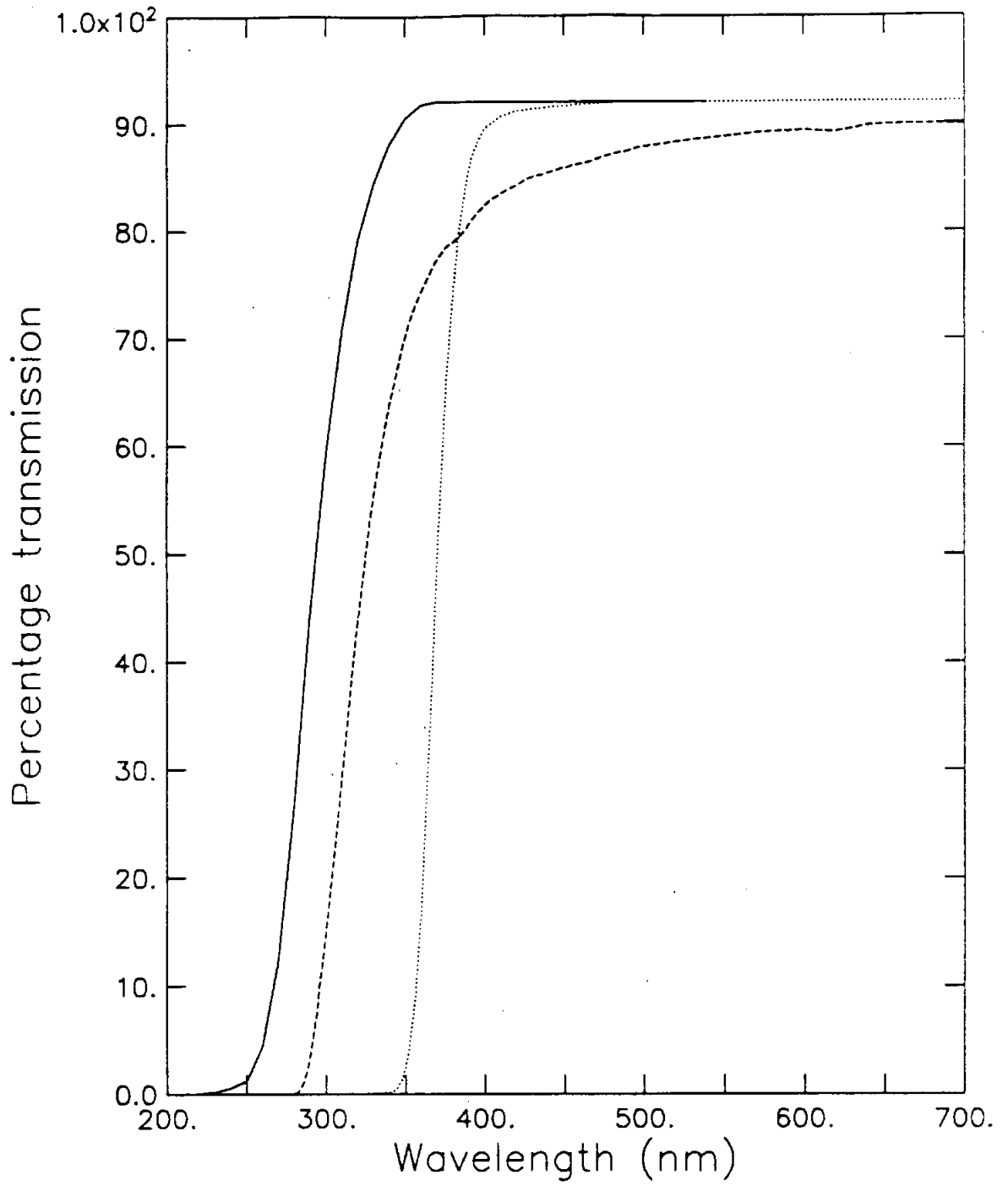
Figure 2: The optical transmission of encapsulation materials. The solid line represents borosilicate glass, the dotted line represents uv-stabilized acrylic, and the dashed line represents high purity non-stabilized acrylic.

Material	Density	Refractive index	Čerenkov threshold
Acrylic	1.181	1.505	173 keV
Water	1.000	1.343	255 keV
Glass	~ 2.5	~ 1.51	~ 171 keV

Table 1: The properties of some Čerenkov media.

was used not only to construct some sources with well-defined spectral intensity, but also to provide filtration when using sources with unknown spectral intensity at short wavelengths. The dashed line in the figure shows the transmission of a 51.0 mm thick sample of 'Polycast' acrylic, which is free from the uv-stabilizer described above. The data clearly show that there is evidence of deviation from the 92 % limit from the 4 % Fresnel reflection at each surface. This could be due to Rayleigh scattering of light due to surface imperfections, but bulk attenuation cannot be ruled out from the data.

It should be noted that only the bulk attenuation length is of interest to the Čerenkov sources described here, as the Fresnel factor does not reduce the light output from a source. A photon reflected at one boundary, will traverse the source and, given no bulk attenuation, have a similar probability of transmission on the opposite side. Since the sources described in this work are (approximately) spherically symmetric, this process is equally likely at all angles, and hence interface reflections may be ignored. This symmetry argument also implies that Rayleigh scattering within the bulk material of the source can be ignored.

The refractive index of the electron stopping medium is clearly important to the simulation of Čerenkov radiation , as both the threshold and rate of photon production are affected by the refractive index. It is quite common to assume that the refractive index of media such as water and acrylic are constant over the range of wavelengths to which bi-alkali cathode photomultipliers are sensitive; between 300 and 700 nm. This is a satisfactory approximation in most cases because the refractive index of such materials changes slowly in this range of wavelengths. However, the effects of the increase of refractive index with decreasing wavelengths are assessed in this study.

In this study it is most important to evaluate the refractive index at the appropriate wavelength, corresponding to that which most photons are counted by a PMT with a bi-alkali photocathode. As demonstrated in the next section, this is about 400 nm. The data set is shown in figure 3, along with a 7th order fit to the data, made for computation purposes. For comparison, the refractive index of water is shown in the figure, denoted by the boxes, from data taken from the Kaye and Laby data book. All data are measured at 20°C. The values of refractive index and density used in the simulations are shown in table 1. Approximate values of these quantities for borosilicate glass are shown in the table.

Source construction

In this section the methods used to construct and fill the sources are described. Sources of three main types were constructed, with some variations within each category. The first types of source were prototypes made from acrylic, but these may be susceptable to radiation damage if large amounts of activity are used for long periods of time. The mark 3 source, constructed from borosilicate glass, proved to be the most successful source. The source was made from a spherical glass bulb of mean diameter 51.14 mm, and average wall thickness approximately
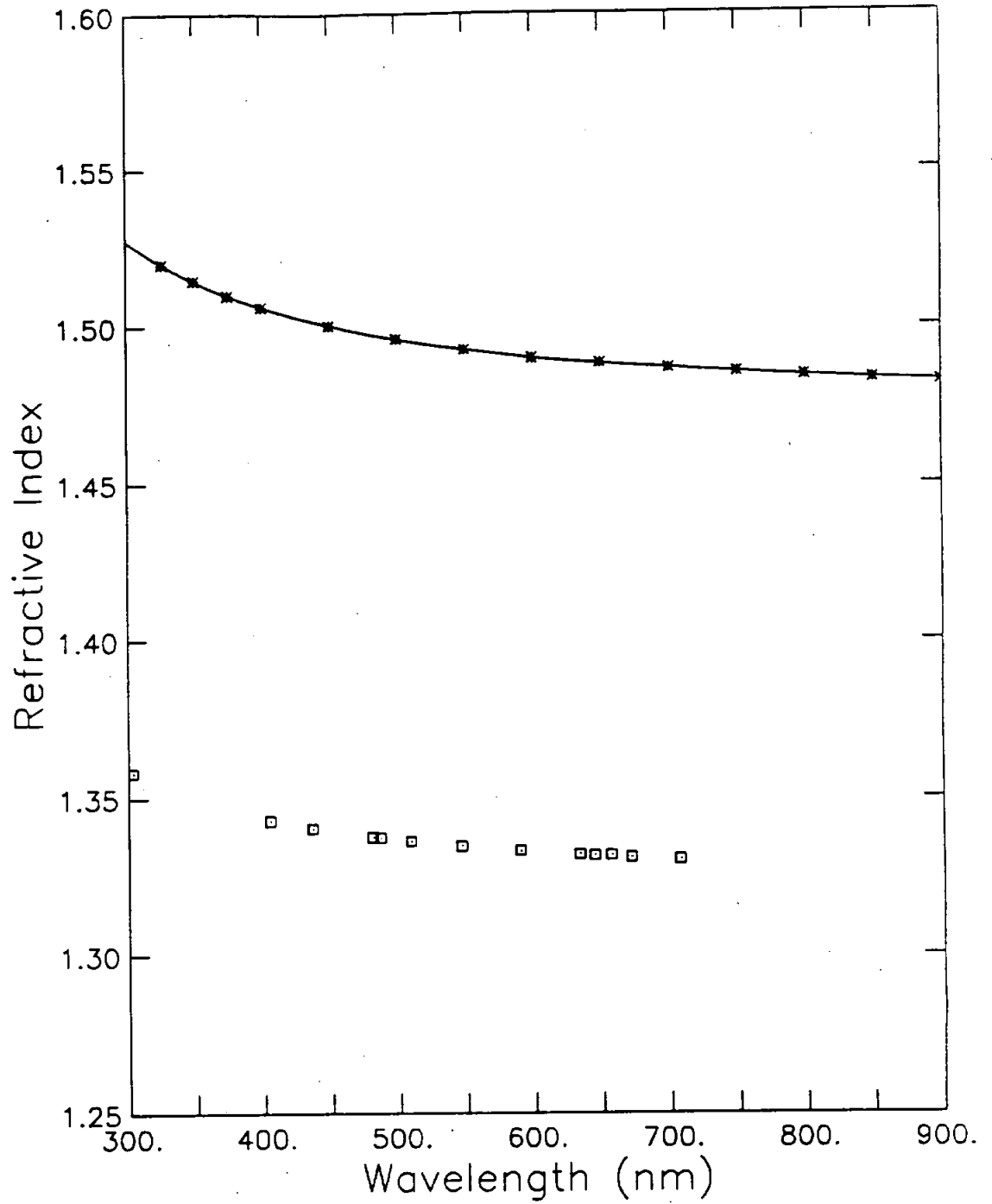
Figure 3: The refractive index of acrylic and water. The points denoted by an ∗ show the refractive index of a Roehm Acrylic without uv-stabilizer, see text for details. The continuous line shows a 7th order fit to the Roehm data. The boxes indicate the refractive index of water.

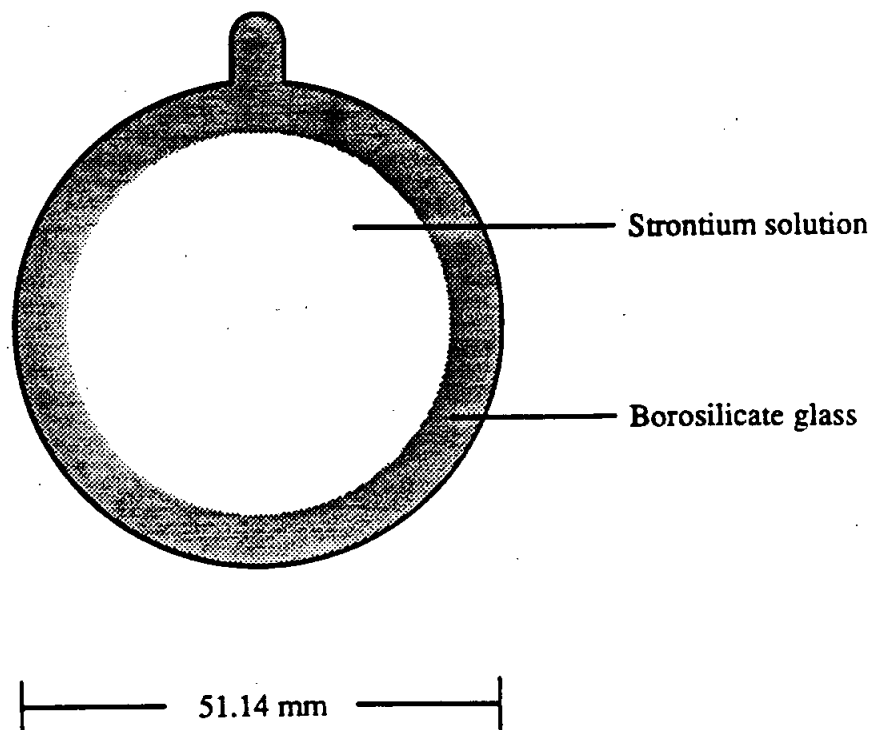| Outer diameter	Wall thickness	Volume of solution	Activity (kBq)
51 mm (avg)	~ 5 mm	36.5 ml	1129.67

Figure 4: The mark 3 source. The activity of ^{90}Sr is quoted on January 8, 1992.

5.0 mm. The source was partially filled with ^{90}Sr dissolved in 0.1 molar hydrochloric acid, and then filled with high-purity water so that air is excluded from the bulb. The source and its construction parameters are shown in figure 4. After filling, the neck of the bulb was sealed by melting the glass near the bulb, and the neck was then cut off to leave a spherical bulb. The advantages of this source over the previous ones are that it will not incur radiation damage, and it has no attenuation of photons for wavelengths longer than about 320 nm. In addition, the use of water as a stopping medium ensures no scintillation light. The activity of ^{90}Sr is over 1 MBq and thus better signal to noise ratios are achieved in photomultiplier calibration experiments. Since the ^{90}Sr plus carrier materials are left in solution, their optical screening effects are reduced. The main simulation results for this source are shown in the rest of the report. The mark 3 source forms the basis for the most accurate determination of the measurement of photomultiplier counting efficiency.

The concentration of the ^{90}Sr solution, 458 kBq per gram of solution, is quoted by the supplier [1] to an accuracy of ± 1.2 % (systematic) ± 0.3 % (random). This measurement is made using a liquid scintillation counter with 4π efficiency, and the measurement technique is accredited by the National Measurement Accreditation Service. The only other radionuclide

---

[1] Amersham International plc.

present in the solution at a significant level (apart from the yttrium daughter) is ^{137}Cs, which represents 14 ppm of the total activity. The specific activity quoted by the supplier is used to deduce the activity in each sphere, with corrections for decay using a half-life of 28.6 ± 0.3 years. The beta spectrum of these decays was computed using Unique first-forbidden decay spectrum corrected for the effects of the Nuclear Coulomb field (Fermi function) and atomic (Rose) screening. Details of the computation are available on request.

Simulation results

Simulations were performed for all three types of source, using both the EGS4 Monte Carlo and an analytic integration method. However, since the mark 3 source has two Čerenkov media, the spatial propagation of the electron is no longer trivial, and simulations of the mark 3 source can only be computed using the Monte Carlo method. Since the mark 3 source is the most likely candidate as the design for a SNO calibration source, only the simulation results of the mark 3 source are reported here. The simulation results of the mark 2 sources are reported in SNO-STR-91-033.

The Monte Carlo analysis presented here does not explicitly deal with the systematic effects of the variation of refractive index with photon frequency. For Čerenkov photons, this effect alters the shape of the Čerenkov spectrum from being constant with respect to frequency to one which rises slowly with frequency. This effect is not negligible for the sources described in this thesis, and if the effect is ignored by choosing an inappropriate frequency at which to evaluate the refractive index, errors of several percent are generated. In the report SNO-STR-91-033, the spectrum of Čerenkov photons is calculated analytically using a refractive index as a function of photon frequency. It has been found that by evaluating the refractive index at a wavelength of about 400 nm, the errors introduced by a constant refractive index are made negligible in comparison with other systematic errors. This can be demonstrated qualitatively by observing that both the Čerenkov spectrum and the quantum efficiency of photomultipliers rise towards the short wavelength range of the spectrum of interest here. The value used for the simulation of the mark 3 source is a value reported in Kaye and Laby, which is n = 1.342742, at a wavelength of 404.66 nm. See figure 3.

The results of the simulation predicts the mean yield $Y(\omega)$ of Čerenkov radiation per beta decay electron from ^{90}Sr and ^{90}Y in solution within the sphere. Table 2 shows the results of the simulation for 300,000 radioactive beta electrons sampled randomly from the ^{90}Sr and ^{90}Y beta spectra, as the two isotopes are assumed to be in equilibrium. Column 3 of the table shows the sensitivity of the yield to the refractive index of water n_w. The fourth column shows the mean electron energy of all the 300,000 decays in the Monte Carlo. The final column shows the fraction of the total Čerenkov radiation which originates from the decays of [90]Sr. In order to address the question of radiation safety, the energy flux of γ rays leaving the sphere was computed in the simulation. The mean energy leaving the sphere was found to be about 2.5 keV per beta decay. However this value is quite sensitive to the internal parameters used in EGS4, and so should be taken as an order of magnitude estimate only.

Decays	$Y \times 10^{-14}$	$dY/dn_w \times 10^{-14}$	Mean e^- energy	f_{Sr}
300,000	1.317 ± 0.004	4.34 ± 0.01	572 ± 1 keV	1.4 %

Table 2: Results of the Monte Carlo simulation of the mark 3 source.

7

Activity	Refractive indices	EGS4	Stopping power	^{90}Y spectrum	Total
1.5 %	1 %	1 %	2 %	1 %	3 %

Table 3: Contributions to the uncertainty of the Čerenkov light yield from the mark 3 source.

The sources of error associated with the final computation of the light output are then listed in table 3. In several cases the values shown are estimates. The EGS4 error figure refers to the total uncertainties from the choice of internal parameters and statistical processes in the Monte Carlo calculation. The error labelled ^{90}Y spectrum, refers to the uncertainties in the shape of the spectrum and its end point energy. The estimate of the total uncertainty assumes that the errors listed in the table are randomly distributed with respect to one another. The conclusion of this simulation is that the absolute value of the yield of Čerenkov radiation from the mark 3 source can be computed to about 3 % accuracy.

The graphs in figure 5 show a sample of electron energies used in the Monte Carlo, and the yield of Čerenkov radiation produced as they stop in the solution and/or the glass envelope. Figure 6 shows a two dimensional projection of the paths of beta decay electrons in the source.

The small contribution to the photon spectrum from internal bremsstrahlung can be approximated by

$$\frac{dN}{d\omega}(\beta,\omega) = \frac{\alpha}{\pi\omega} f(\beta), \tag{1}$$

where $f(\beta)$ is a model dependent function of the initial electron velocity βc. This function $f(\beta)$ is of order unity for relativistic beta decays, and vanishes as $\beta \to 0$. At wavelengths in the ultra-violet region, the contribution from the internal bremsstrahlung photon spectrum is about 4 orders of magnitude below the Čerenkov light output shown in table 2, and so no correction is made. In a similar manner the photon flux from external bremsstrahlung can be shown to be negligible for these sources.

Outlook

The plans to include such a source of Čerenkov radiation in the calibration of the SNO detector rely on making several slight modifications to the basic design reported here. The safety of the source, and in particular its structural integrity, have to be assessed more fully. A more detailed study of the radiation damage problem is required as more activity (at least 10 MBq) will be needed in a SNO source. If the source is to be used in the light water region between the PSUP and the acrylic vessel, then the source should be constructed from quartz instead of glass. This is necessary as the transmission of the acrylic no longer dominates the spectral intensity visible to the photomultipliers.
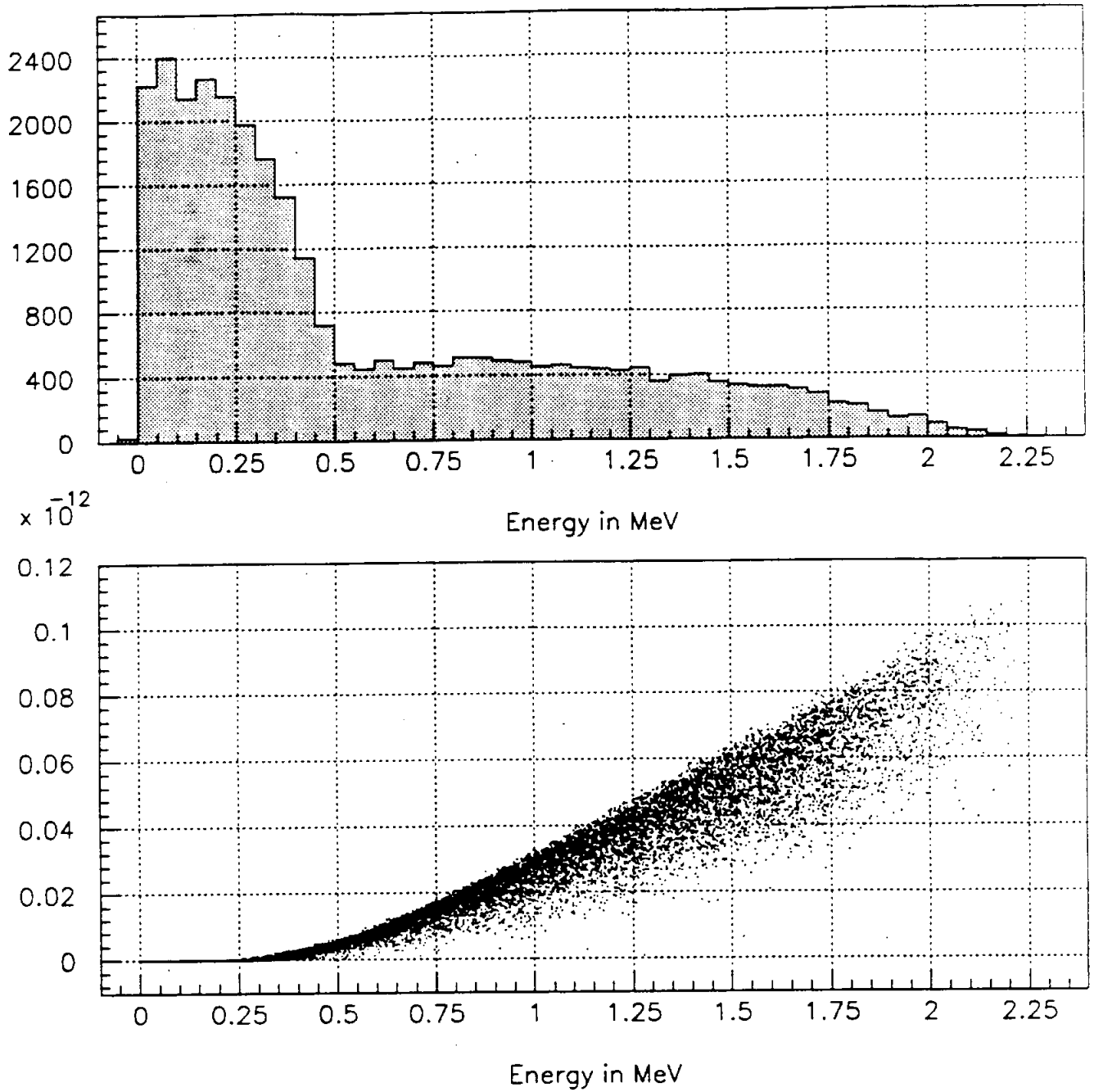
Figure 5: The upper histogram shows a sample of initial electron kinetic energies from the beta spectra of ⁹⁰Sr and ⁹⁰Y. The scatter plot shows the yield of Čerenkov radiation from electrons of various energies.
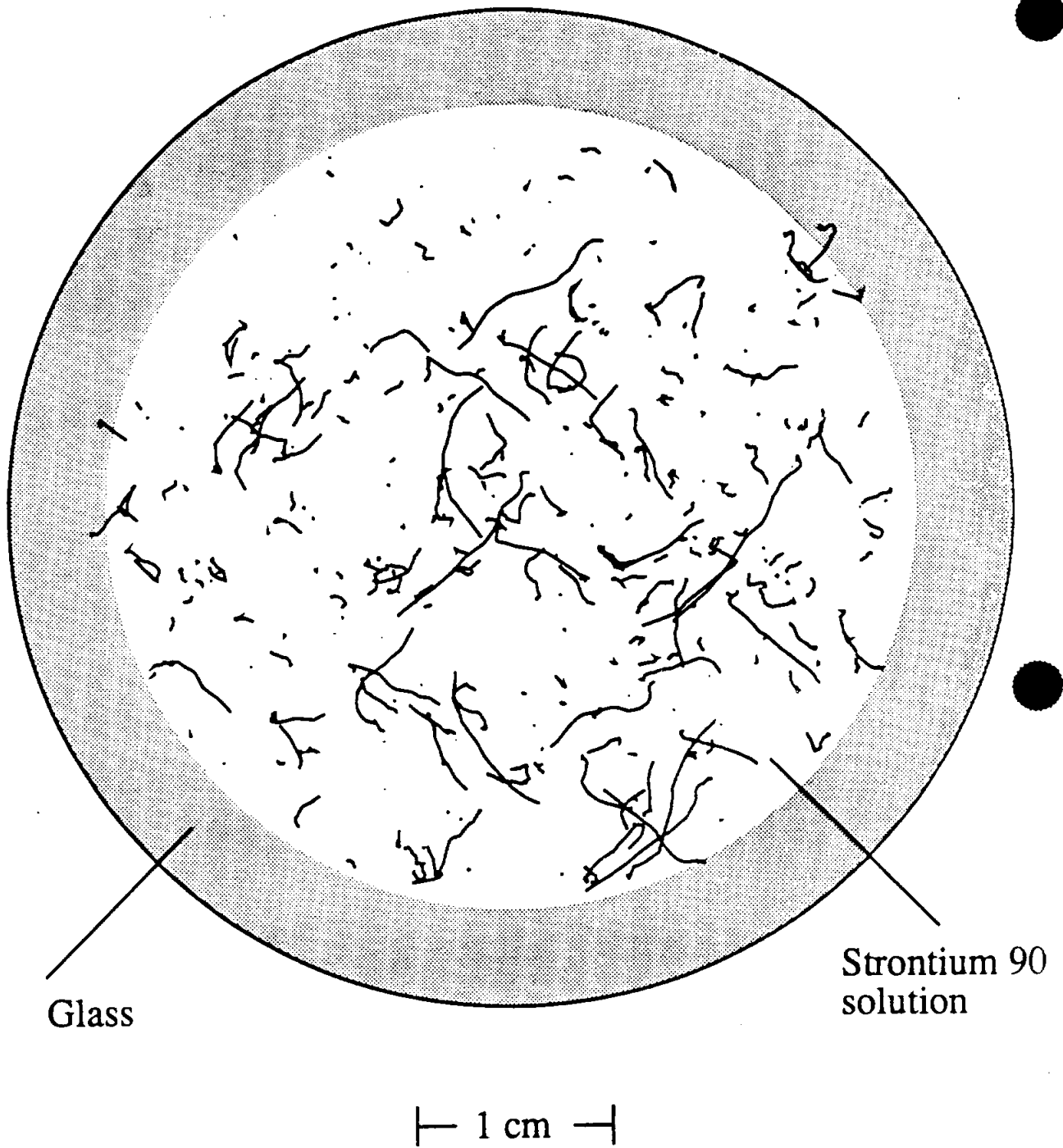
├─ 1 cm ─┤

Figure 6: Projection of beta decay electron trajectories in the mark 3 source.